Running Title

ACD1 is involved in oxygenation of pheophorbide *a*

Corresponding author: Ryouichi Tanaka

Institute of Low Temperature Science, Hokkaido University, Kita-ku, N19 W8, Sapporo, 060-0819, Japan

tel: +81-11-706-5496, fax: +81-11-706-5493

e-mail: rtanaka@lowtem.hokudai.ac.jp

Subject areas: proteins, enzymes and metabolism

Number of figures: 6

Number of tables: 0

Number of pages: 40

Title: The *Arabidopsis-accelerated cell death* gene *ACD1* is involved in oxygenation of pheophorbide *a*: Inhibition of the pheophorbide *a* oxygenase activity does not lead to the "stay-green" phenotype in *Arabidopsis.*

Authors: Ryouichi Tanaka[1], Masumi Hirashima[1], Soichirou Satoh[2], Ayumi Tanaka[1]

[1]Institute of Low Temperature Science, Hokkaido University, and CREST, Japan Science and Technology Corporation, Kita-ku, N19 W8, Sapporo 060-0819, Japan,

[2]Institute of Low Temperature Science, Hokkaido University, Kita-ku, N19 W8, Sapporo 060-0819, Japan

Abbreviations: chlorophyll, Chl; choline monooxygenase, CMO; chlorophyllide *a* oxygenase, CAO; pheophorbide *a* oxygenase, PaO; red chlorophyll catabolite, RCC; fluorescent chlorophyll catabolite, FCC; primary fluorescenct chlorophyll catabolite, pFCC

Abstract

Oxygenation of pheophorbide *a* is a key step in chlorophyll breakdown. Several biochemical studies have implicated that this step was catalyzed by an iron-containing and ferredoxin-dependent monooxygenase, pheophorbide *a* oxygenase (PaO). It has been proposed that inhibition of its activity arrests the chlorophyll breakdown and leads to the "stay-green" phenotype. We searched the *Arabidopsis* genome for a possible PaO encoding gene and hypothesized that it has homology to known iron-containing Rieske-type monooxygenase sequences. We identified three such open reading frames, Tic55, ACD1 and ACD1-like. We produced transgenic *Arabidopsis* plants which expressed antisense RNA as a method to inhibit the expression of these genes. The appearance of these antisense plants were indistinguishable from that of the wild type under illumination. However, after they were kept under darkness for 5 days and again illuminated, the leaves of the antisense ACD1 plants (AsACD1) were bleached. Leaves of AsACD1 accumulated 387 nmol/gram fresh weight pheophorbide *a* which corresponded to 60 % of chlorophyll *a* degraded. The rate of decrease in chlorophyll *a* was not influenced in senesced AsACD1 leaves. These results demonstrated that

ACD1 is involved in PaO activity, and its inhibition led to photooxidative destruction of the cell instead of the "stay-green" phenotype.

Introduction

Degradation of chlorophylls (Chls) is a developmentally-regulated and programmed cellular process usually related with leaf senescence. It is important to understand the molecular basis for Chl catabolism, as it could influence the entire process of leaf senescence. Intermediate products of Chl catabolism are potentially toxic to cells, as they absorb light and may generate radical oxygen species that ultimately lead to necrotic cell death (e.g. Mach et al. 2001, Jonker et al. 2002). Thus, once the breakdown of Chls is onset, the products should be rapidly catabolized by coordinated actions of multiple enzymes. Additionally, as Chls stabilize membrane-bound photosynthetic proteins, their degradation plays a key role in initiation of mobilization and recycling of nitrogen stored as part of photosynthetic proteins (Thomas et al., 2002).

Angiosperms have two chlorophyll species, Chl *a* and Chl *b*. Upon senescence, Chl *b* is converted to Chl *a* by Chl *b* reductase and 7-hydroxymethyl Chl reductase (Ito et al., 1993; Ito et al., 1994; Ito et al., 1996; Scheumann et al., 1996; Scheumann et al., 1998). Therefore, only Chl *a* enters the Chl catabolic pathway (For

a review, see Matile et al., 1999). First, the phytol chain of Chl *a* is removed from its porphyrin ring to produce chlorophyllide *a* by chlorophyllase (Tsuchiya et al., 1999; Jacob-Wilk, 1999). Second, the Mg ion of chlorophyllide is removed by Mg-dechelatase to generate a green color pigment, pheophorbide *a* (Vicentini et al., 1995b; Shioi et al., 1996). Third, the macrocyclic ring of pheophorbide *a* is cleaved by pheophorbide a oxygenase (PaO) to generate a red color pigment, the red chlorophyll catabolite (RCC, Wüthrich et al., 2000). RCC is further catabolized to primary fluorescent Chl catabolites (pFCCs), FCC and non-fluorescent Chl catabolites (NCCs). All the catalytic steps except for the conversion of FCCs to NCCs take place within a specialized form of a plastid, termed a gerontplast (for reviews, see Matile et al., 1996; Matile et al., 1999; Takamiya et al., 2000).

Among the enzymes mentioned above, PaO draws special attention from plant researchers in relation to the "stay-green" phenotype. Thomas et al. (1989) investigated a stay-green mutant of *Fetsuca platensis*, Bf993 and found an unusual accumulation of chlorophyllide *a* and pheophorbide *a*. Vicentini et al. (1995a) discovered that among the enzymatic activities from Chl *a* to RCC, only the PaO

activity is missing in this mutant. These findings led to a hypothesis that suppression of the PaO activity allowed the plants to "stay green" (Matile et al., 1999, Thomas and Howarth, 2000). Thomas and Howarth (2000) proposed that stay-green mutants can be categorized into five groups according to their phenotypes. Based on their proposal, mutants that have a defect in the chlorophyll breakdown pathway fall into Type C stay-greens. Within these type C stay-greens, the contents of Chls remain constant during senescence while carbon fixation activities are lost. In addition to Bf995, the *cytG* mutant of soybean (Guiamet et al., 2002) and a non-yellowing cultivar of *Dendranthema grandiflora* (Reyes-Arribas et al. 2001) might be classified into this type. Retention of Chls and Chl-binding light-harvesting proteins during senescence was observed in these mutants.

Extensive biochemical studies revealed several features of PaO. The enzyme is an iron-containing monooxygenase that requires reduced ferredoxin and NADPH to function (Curty et al., 1995; Hörtensteiner et al., 1995; Hörtensteiner, et al., 1998). The PaO activity was mainly observed in envelope membranes of gerontplasts (Matile and Schellenberg, 1996).

Completion of the genome sequencing project of *Arabidopsis* (Arabidopsis Genome Initiative, 2000) enabled us to search the database for putative PaO encoding genes. We identified three possible PaO encoding genes, which were designated *Tic55*, *Accerelated-cell-death 1* (*ACD1*) and *ACD1-like*. Using the antisense RNA technique, we examined involvement of these genes in PaO activity. Our observation with antisense *ACD1* transgenic plants clearly demonstrated involvement of ACD1 in PaO activity. Inhibition of PaO activity resulted in a severe photo-oxidative damage rather than the stay-green phenotype.

Results

Search for possible PaO encoding genes

As previously mentioned, biochemical studies revealed several features of PaO. It was predicted to be a iron-containing ferredoxin-dependent monooxygenase localized in plastids (Curty et al., 1995, Hörtensteiner et al., 1998). We hypothesized that the possible PaO genes encode an iron-binding motif, a transit peptide for plastids and probably a Rieske-type iron-sulfur center for efficient transfer of electrons from a

ferredoxin protein. We found multiple sequences which fulfilled these criteria. The sequences were then categolized according to their phylogenetic relationships (Fig. 1) and delineated into 5 distinct clades. The function of proteins in the choline monooxygenase (CMO) and the chlorophyllide *a* oxygenase (CAO) clades have already been clearly assigned. CMO functions to catalyze the synthesis of betaine-aldehyde (Rathinasabapathi et al. 1997) and whereas CAO functions to catalyze the synthesis of chlorophyllide *b* (Tanaka et al. 1998, Oster et al. 2000). Tic55 (At2g24820), *Accelerated cell death 1 (ACD1)* (At3g44880) and an *ACD1*-like gene (At4g25650) all belong to a divergent mono- and di-oxygenase superfamily containing a Rieske-type 2Fe-2S center as well as a non-heme mononuclear iron binding site (Schmidt and Shaw, 2001). Tic55 was first isolated as a component of translocons which is located in inner envelope membranes (Caliebe et al. 1997). Although it was proposed to be involved in redox-regulated protein transport (Kuchler et al. 2002), its exact function is still unknown (Reumann and Keegstra, 1999, Heins et al. 2002). ACD1 was first cloned from a mutant which exhibited enhanced cell-death responses to pathogens and abnormal patterns of leaf senescense (Greenberg and Ausubel, 1993). The ortholog of

ACD1 in maize (*Zea mays*) is called *Letha- leaf-spot 1 (Lls1)* (Gray et al., 1997). Gray et al. (2002) reported that various biotic and abiotic agents cause formation of necrotic spots in a *lls1* mutant in a light-dependent manner. This is a characteristic feature of mutants that accumulate the intermediate compounds of porphyrin metabolism (Kruse et al. 1995, Mock and Grimm, 1997, Hu et al. 1998, Papenbrock et al. 2001, Mach et al. 2001). However, accumulation of porphyrin compounds in *lls1* or *acd1* mutants have not reported. ACD1 (Lls1) protein is predicted to be localized in plastids (Gray et al., 2002). The ACD1-like genes were found in the *Arabidopsis* and rice genomes, and alludes to a universal role of the gene products in angiosperms. Concurrently, to Lls1 protein localization, computer-assisted analysis with TargetP software (Emanuelsson et al. 2000) predicted that the ACD1-like protein also localizes in plastids (data not shown).

Dark to light transition caused cell death in antisense ACD1 plants

In order to asses the function of these gene products, we produced transgenic

Arabidopsis plants in which antisense RNA for Tic55, ACD1 or ACD1-Like is constitutively expressed under the control of the cauliflower mosaic virus 35S promoter. These plants were indistinguishable from wild-type plants under continuously illuminated conditions (Fig. 2A, 2D, 2G, 2J). However, when these plants were transferred to darkness, slight differences in morphology were observed (Fig. 2B, 2E, 2H, 2K). Leaves of the wild-type plants (Fig. 2B) and antisense Tic55 (AsTic55; Fig. 2E) and antisense ACD1-Like plants (AsACD1-Like; Fig. 2K) gradually turned yellow in darkness. In contrast, the leaves of the antisense ACD1 (AsACD1) plants remained greenish after 5 d of dark treatment (Fig. 2H). This pattern continued even when they were kept in darkness for 9 d (data not shown), but their leaves were unusually waved and were appeared to be dehydrated (Fig. 2H). The appearance of AsACD1 leaves was very similar to that of *acd2* mutants that have a defect in their RCC reductase activities (Mach et al., 2001). The difference between these transgenic plants became more apparent when they were returned to illumination. The appearance of the wild-type, AsTic55 and AsACD1-Like plants remained unchanged (Fig. 2C, 2F, 2L). However, leaves of AsACD1 turned white and dried after 24h (data not shown) to 72 h

(Fig. 2I) of illumination. It should be noted that all the leaves exposed to this dark-light treatment did not recover, but new leaves appeared from the meristem a few days after transition from dark to light. These data indicate that the meristematic tissue was not severely damaged by this dark-light treatment.

Accumulation of pheophorbide a in the antisense plants

It is well known that porphyrin compounds that are not associated with cognate proteins generate reactive oxygen species upon illumination. Light-dependent bleaching of leaves was commonly observed in mutants in that exhibited defective tetrapyrrole metabolism as described above. The phenotype of AsACD1 suggested that this plant accumulated porphyrin compounds during dark treatment. We extracted pigments from these transgenic plants and analyzed their composition by HPLC (Fig. 3; only representative data for wild type and AsACD1 was presented). A clear difference was observed in leaves of AsACD1 and other plants in their pheophorbide *a* contents (Fig 4). Up to 7.8 nmol/gFW pheophorbide *a* was accumulated in the wild-type, AsTic55 and AsACD1-like plants, whereas 387 nmol/gFW pheophorbide *a* was accumulated in AsACD1 plants (Fig. 4). The contents in other pigments were not significantly

different in these plants (Fig. 3). With the exception of protochlorophyllide and chlorophyllide, which was accumulated to a small amount (less than 1% of the Chl *a* contents) in both wild type and AsACD1, we could not detect protoporphyrin IX, Mg-protoporphyrin IX or other photosensitizing porphyrin intermediates of the Chl biosynthetic pathway. These results indicated that antisense suppression of *ACD1* gene expression did not influence the biosynthetic steps of Chls. Accumulation of RCC was analyzed by HPLC according to the method of Rodoni et al. (1997). In our experience, we have not detected accumulation of RCC in both the wild-type and AsACD1 plants (data not shown). These results indicated that pheophorbide *a* accumulation caused bleaching of the leaves in AsACD1 plants.

In our next step, we examined the time-course of pheophorbide *a* accumulation and its relationship with the photo-bleaching phenotype of AsACD1. After 3 d of dark treatment, 106 nmol/gFW of pheophorbide *a* accumulated in AsACD1 and it increased to 251 nmol/gFW after 5 d, whereas only 1.14 nmol/gFW pheophorbide *a* at its maximum was detected after 3 d in wild type. The accumulation of pheophorbide *a* in AsACD1 leaves was in parallel with that of Chl breakdown (Fig. 5).

It is likely that the Chl catabolic pathway was blocked at the step of pheophorbide *a* oxygenation. Approximately, 30% of Chls were lost during dark incubation for 5 d in both wild type and AsACD1 (Fig. 5). Almost 60% of degraded Chls were accumulated in the form of pheophorbide *a* in AsACD1 during 5 d of dark incubation. The rate of Chl breakdown was similar in both plants (Fig 5).

Changes in plastid structure upon dark-light treatment in AsACD1

Leaf damage in AsACD1 after dark-light transition was not apparent until 24 hrs of re-illumination. However, if the cellular damage was caused by pheophorbide *a* accumulation, its photo-bleaching effects should have occurred earlier, especially in plastids where pheophorbide *a* is expected to accumulate. As a result, we next examined the ultrastructure of the cells before damage of leaves became evident in AsACD1 plants.

Cell ultrastructure was totally indistinguishable under continuous illumination. Chloroplasts in both the wild-type and AsACD1 plants were ovoid and contained well-developed grana structure (Fig. 6 A and B). After they were remained under

darkness for 5 d, the grana structure was still retained in both plants (Fig. 6C, 6D). The shape of the chloroplasts was rather spherical, indicating that re-organization of the cytoskeleton holding the chloroplast structure was proceeding under darkness.

Striking difference was observed after the plants were re-illuminated. Chloroplasts of wild type regained normal-shaped well-organized grana structure (Fig. 6E). On the other hand, grana structure in AsACD1 was totally destroyed (Fig. 6F). In addition, chloroplast and cell shape was completely distorted in AsACD1. Six hours after transition from darkness to light, stroma lamella structure was still observed in AsACD1 (Fig. 6F), but after 24 h of illumination all cellular components seemed to be destroyed (Fig. 6H). As pheophorbide *a* is well-known as a strong photo-sensitizer (e.g. Jonker et al. 2002), its accumulation might have generated reactive oxygen species. This would have an affect on the permeability of membranes to distort the shapes of chloroplasts and cells in AsACD1 plants.

Discussion

In this study, we demonstrated that repression of *ACD1* expression led to unusual pheophorbide *a* accumulation in a senescence dependent manner (Fig. 5). Pheophorbide *a* accumulation ultimately caused cell death after dark-light transition through its photo-sensitizing properties (Fig. 2 and Fig. 6). During 5 d of dark incubation, 30% of Chl *a* was degraded, and almost 60% of it was accumulated as phoephorbide *a* in the AsACD1 plants. These results clearly demonstrated that ACD1 is involved in oxygenation of pheophorbide *a*. The amino acid sequence of ACD1 contains a putative transit peptide sequence, a rieske domain and a mono-nuclear iron binding domain (Gray et al., 2002). It belongs to a divergent mono- and dioxygenase superfamily distributed among various bacteria and plants (Gray et al., 2002). Some of the enzymes in this superfamily show ring fission activities (Mason and Cammack, 1992). The leaves of AsACD1 were waved and dehydrated after dark treatment. This phenotype resembles that of a *acd2* mutant which has a defect in the RCC reductase gene (Mach et al. 2001). These observations strongly indicate that ACD1 is the catalytic component of PaO.

In wild-type and AsACD1 plants grown under continuous illumination,

accumulation of pheophorbide *a* was negligible (Figs 4 and 5). It was consisted with the observation that Chls only turnover upon senescence or in stressful conditions (Beale and Weinstein, 1990). During forced leaf senescence which was caused by dark treatment, approximately 60% of the Chls degraded were accumulated as pheophorbide *a* (Fig. 5). These data indicated that the Chl breakdown pathway in which PaO is involved primarily operates in this period, whereas another pathway that might occur outside plastids (Takamiya et al., 2000) does not play a major role in this condition. Further, cell death lesion formation was observed in AsACD1 (data not shown) and in an *acd1* mutant (Greenberg and Ausubel, 1993) during normal leaf aging. This observation indicated that the PaO pathway of chlorophyll breakdown plays a dominant role in Chl degradation in normal leaf aging as well as in forced leaf senescence.

The *Arabidopsis ACD1* was first identified as the mutant gene, which caused an enhanced cell death response to pathogen infection (Greenberg and Ausubel, 1993). A mutation in the *leathal leaf spot1* gene, the maize ortholog of *ACD1*, also caused formation of necrotic spots as a result of various biotic and abiotic stresses (Gray et al., 1997; Gray et al., 2002). These mutant phenotypes may be the consequence of

chlorophyll breakdown induced by various biotic and abiotic stresses as well as subsequent accumulation of pheophorbide *a* by *acd1* or *lls1* mutation. A similar scenario was observed in *acd2* mutants in which defects in the RCC-reductase encoding gene caused accumulation of RCC and enhanced response to pathogen infection (Mach et al. 2001). Further investigation would be required to confirm whether or not the chlorophyll breakdown process is involved in some of the pathogen response including the hypersensitive response, as it was hypothesized during the screening of *acd* or *lls* mutants.

Accumulation of pheophorbide *a* did not lead to a decrease in the rate of Chl degradation in AsACD1 plants. This observation indicates that the chlorophyll catabolic pathway is not regulated by a feedback mechanism involving pheophorbide *a* accumulation, as hypothesized by Matile et al. (1999). Rather, at least in *Arabidopsis* it appeared to be potentially hazardous for plant cells to control the pathway at the step of PaO as it might increase a possibility to accumulate pheophorbide *a* (see Figs. 2 and 6). As the first irreversible step of the chlorophyll catabolic pathway is de-chelation of Mg, this step could be the regulatory point of this pathway. Otherwise, transfer of the

Chl-binding proteins from thylakoid membranes to envelope membranes where the Chl catabolic activities are primarily found might trigger the breakdown of Chls. This transfer mechanism of the proteins from this direction is largely unknown, but involvement of VIPP1 protein in the transfer mechanism to the opposite direction was recently uncovered (Kroll et al. 2001). A similar mechanism in which VIPP1 protein is involved might operate at the first step of Chl breakdown. The phenotype of Type C stay-greens (Thomas and Howarth, 2000) might be interpreted if assuming a defect in such a transfer system from thylakoid to envelope membranes and its possible "feed forward" effects on the PaO activity.

In conclusion, this study demonstrated that ACD1 is involved in the PaO activity. Accumulation of pheophorbide *a* caused severe damage to AsACD1 leaves. This would infer that tight regulation of chlorophyll catabolic enzymes is required during leaf senescence. Further studies on PaO and its regulatory system are warranted and provide important clues to understanding the entire process of leaf senescence.

Materials and Methods

Plant Material and Growth Conditions

Arabidopsis thaliana (Columbia ecotype) was grown for 3 weeks in a chamber equipped with white fluorescent lamps (FLR40SSW, NEC Co. Ltd., Tokyo, Japan) under continuous illumination at a light intensity of 100 μE m^{-2} s^{-1} at 22 ºC on a 1:1 mixture of vermiculite and nourished soil (Sankyo-Baido soil, Hokkai-Sankyo Co. Ltd., Kita-Hiroshima, Japan). The plants were subsequently transferred into darkness for 1 to 5 d at 22 ºC and returned to the light conditions as described above. The third whorl of leaves was harvested at the time indicated in the result section and immediately frozen in liquid nitrogen for pigment analysis. For electron microscopy, the fourth whorl of leaves counting down from the top of the plant was harvested and immediately soaked in the primary fixation solution (1% paraformaldehyde, 2.5% glutaraldehyde in 50 mM PIPES buffer, pH 7.2 containing 0.1 M sucrose).

Biocomputational analysis

The neighborhood search algorithm BLAST (Altschul et al., 1990) was employed for database searches using the World Wide Web BLAST servers of the National Center for

Biotechnology Information (NCBI). The accession numbers of the amino acid sequences used for construction of the phylogenetic tree were listed in the legend for Fig. 1. Putative open reading frames were aligned using of the ClustalX (Thompson et al. 1997) with the Gonnet matrix with gaps. After alignment, the sequences were trimmed so that those corresponding to *Arabidopsis* ACD1 from 100Asn to 412Gln were realigned and used for the phylogenetic analysis by the neighbor joining method (Saitou and Nei, 1987). Unrooted cladograms were generated by using the TreeViewPPC version 1.6.6 program. The bootstrap method (Felsenstein 1985) was performed for 1,000 replicates.

Construction of the transgenic plants

Total RNA was extracted from 3-week-old *Arabidopsis* leaves using RNeasy Plant Mini Kit (Qiagen GmbH, Hilden, Germany) and reverse transcribed by a reverse transcriptase, ReverTra Ace, (Toyobo Co. Ltd., Osaka, Japan) to cDNA according to the manufacturer's instructions. Using this cDNA aliquot as the PCR template, the full coding regions for Tic55 (At2g24820), ACD1 (At3g44880) and ACD1-like

(At4g25650) proteins were amplified using Pfu DNA polymerase (Toyobo). For transformation of *Arabidopsis*, pGreenII vector (Hellens et al. 2000a, Hellens et al. 2000b) was modified as follows. The amplified cDNA fragments were first incorporated between the NcoI and NotI sites of the 35SrsGFP vector (kindly provided by Dr. Niwa in Univ. Shizuoka), then the DNA fragments between the HindIII and EcoRI sites were transferred to the corresponding sites of the pGreenII vector. In the following order, the constructs contained the cauliflower mosaic virus 35S promoter, the omega sequence (Gallie, 2002), antisense-oriented cDNA fragments and NOS terminator. The constructs were transformed into *Agrobacterium tumefaciens* by electroporation. Four-week-old *Arabidopsis* plants (ecotype Columbia) were transformed by the vacuum infiltration method as described by Bechtold et al. (1993). In this study, F3 transformants of 3 independent lines were used. As the phenotypes of these lines were essentially same, we presented here results from one representative line.

Pigment analysis

A leaf was weighed and grinded in acetone using a ShakeMaster grinding apparatus

(BioMedical Science Co. Ltd., Tokyo, Japan). Extracts were centrifuged for 5 min at 10,000 x g and the supernatant was mixed with water so that the final acetone concentration became 80%. According to the method of Zapata et al. (2000), pigments were separated on a reversed phase column, Symmetry C8 (150 x 4.6 mm, Waters) using Ezchrome Elite HPLC system (Hitachi Co. Ltd., Tokyo, Japan) equipped with the photodiode array detector L2450 (Hitachi). Pigments were identified by their spectral patterns and/or co-injection with standards. Pheophorbide *a* was purchased from Wako Chemicals (Tokyo, Japan). Chls were purchased from Juntec Co. Ltd. (Kanagawa, Japan). Pigment quantifications were performed at 665 nm.

Electron microscopy

Arabidopsis leaves were harvested under dim green light and immediately soaked in the primary fixation buffer described above. Samples were rinsed in 50 mM PIPES buffer (pH 7.2, three 15-min rinses) and subsequently dehydrated in a graded series of ethanol dilutions (30, 50, 70, 90, 100 x 3, v/v) for 15 min at each dilution. Samples were embedded in epon resin mixture (TAAB Epon 812, TAAB Laboratories Equipment Ltd,

Berkshire, UK). Ultra-thin sections were mounted on 100-mesh size grids. Specimens were stained for 20 min with 2% (w/v) aqueous uranyl acetate and briefly with lead citrate, washed under a gentle stream of water and viewed with a JOEL 1200EX transmission electron microscope (JOEL Ltd., Tokyo, Japan) operating at 100 kV.

Acknowledgments

We thank Dr. Yasuo Niwa (University of Shizuoka, Japan) for his providing 35SrsGFP vector. We also thank Drs. Roger Hellens and Phil Mullineaux (John Innes Centre, UK) for providing the pGreen vector kit. We would like to acknowledge Dr. Megumi Moriya for her excellent technical assistance in electron microscopy. This work was supported in part by a Research Fellowship for Young Scientists from the Japan Society of the Promotion of Science to S.S., and in part by Grants-in-Aid (No. 15770020) to R. T. from the Japanese Ministry of Education, Culture, Sports, Science and Technology.

Figure Legends

Fig. 1 Phylogenetic relationship between various plant monooxygenase sequences. Plant monooxygenase sequences containing an iron-binding site and a Rieske-type iron-sulfur cluster were selected from the Genbank database and their phylogenetic relationship was deduced by the neighbor joining method. These sequences were classified into five clades, the choline monooxygenase (CMO) clade, the chlorophyllide a oxygenase (CAO) clade, the ACD1 clade, the ACD1-like clade and the Tic55 clade. For all the clades, the calculated bootstrap values calculated from 1000 trials were 100%. The sequences used for the production of antisense plants in this study were indicated in bold letters. Sequences used for the phylogenetic analysis were deposited in Genbank under the following accession numbers: NM_114357 (*Arabidopsis* AtACD1), T04136 (Maize lls1), AAK98735 (Rice lls1), AAL32300 (Tomato lls1), AAP13565 (Cowpea lls1), AL050400 (*Arabidopsis* AtACD1-like gene), AAP21408 (Rice putative cell death suppressor protein, ACD1-like 1), AAP21411 (Rice putative cell death suppressor protein, ACD1-like2), NP_175088 (*Arabidopsis* CAO), BAA82479 (Rice CAO), BAA82480 (liverwort CAO), BAA82481 (*Dunaliella* CAO),

BAA33964 (*Chlamydomonas* CAO), BAA82483 (*Prochloron* CAO), AB021313 (*Prochlorothrix hollandica* CAO), NP_180055 (*Arabidopsis* Tic55), T06499 (Pea Tic55), AK105616 (Rice Tic55), T08550 (*Arabidopsis* CMO), T09214 (Spinach CMO), T14542 (Beet CMO).

Fig. 2 Effects of light-dark-light transitions on the wild-type, AsTic55, AsACD1 and AsACD1-like plants. Phenotypes of wild type (A, B, C), AsTic55, (D, E, F), AsACD1 (G, H, I), and AsACD1-like (J, K, L.) Plants were grown under continuous illumination for 3 weeks (A, D, G, J), incubated under darkness for 5 d (B, E, H, K), transferred again into the light condition and mainteind for 72 hrs under constant illumination (C, F, I, L).

Fig. 3 HPLC chromatograms for wild type and AsACD1 obtained at 410 nm wavelength. Arrows indicate the positions where some representative intermediate compounds of tetrapyrrole biosynthesis are expected to elute. Peaks whose names were not indicated in the chromatograms were from carotenoid derivatives.

Fig. 4 Pheophorbide *a* accumulation in the wild-type, AsTic55, AsACD1 and AsACD1-like plants. Plants were grown for 3 weeks under continuous illumination and under darkness for 5 d. The third whorl of leaves from the top were harvested and analyzed for their phoephorbide *a* contents as described in the “Materials and methods”. Vertical bars represent SE (n = 3).

Fig. 5 Time course of Chl *a* degradation and pheophorbide *a* accumulation during dark incubation. The wild-type and AsACD1 plants were grown for 3 weeks under continuous illumination and incubated under darkness for the time indicated in the graph. The third whorl of leaves was harvested and their pigment compositions were analyzed. Vertical bars represent SE (n = 3).

Fig. 6 Electron-microscopic observation of chloroplast structure in wild type and AsACD1. Chloroplasts of wild type (A, C, E, G) and AsACD1 (B, D, F, H). Plants were grown under continuous illumination for 3 weeks (A, B), incubated under darkness for 5 d (C, D), transferred again to illumination and kept for 6 hrs (E, F) or 24

hrs (G, H). Bars = 1 μm.

References

Altshul, S. F., Gish, W, Miller W., Myers, E. and Lipman, D. (1990) Basic local alignment search tool. *J. Mol. Biol.* 215: 403-410

Arabidopsis Genome Initiative (2000) Analysis of the genome sequence of the flowering plant *Arabidopsis thaliana*. *Nature* 408: 796-815

Beale, S. I., and Weinstein, J. D. (1990) Tetrapyrrole metabolism in photosynthetic organisms. *In* Biosynthesis of heme and chlorophylls. Edited by Dailey, H. A. pp 287-391. McGraw-Hill, New York.

Bechtold, N., Ellis, J. and Pelletier, G. (1993) *In planta Agrobacterium* mediated gene transfer by infiltration of adult *Arabidopsis thaliana* plants. *C. R. Acad. Sci. Paris. Life Sci*. 316: 1194-1199

Caliebe A, Grimm R, Kaiser G, Lubeck J, Soll J and Heins L. (1997) The chloroplastic protein import machinery contains a Rieske-type iron-sulfur cluster and a mononuclear iron-binding protein. *EMBO J*. 16: 7342-7350.

Curty C, Engel, N and Gossauer A (1995) Evidence for a monooxygenase-catalyzed primary process in the catabolism of chlorophyll. *FEBS Lett*. 364: 111-123

Emanuelsson, O., Nielsen, H, Brunak, S and von Heijne, G. (2000) Predicting subcellular localization of proteins based on their N-terminal amino acid sequence. *J. Mol. Biol.* 300: 1005-1016

Felsenstein J (1985) Confidence limites on phylogenies: An approach using the bootstrap. *Evolution* 39: 783-791

Gallie, D. R. (2002) The 5'-leader of tobacco mosaic virus promotes translation through enhanced recruitment of eIF4F. *Nucleic Acid Res.* 30: 3401-3411

Gray J., Close P. S., Briggs, S.P. and Johal, G. S. (1997) A novel suppressor of cell death in plants encoded by the Lls1 gene of maize. *Cell* 89: 25-31

Gray, J., Janick-Buckner, D., Buckner, B., Close, P. S. and Johal, G. S. (2002) Light-dependent death of maize lls1 cells is mediated by mature chloroplasts. *Plant Physiol.* 130: 1894-1907

Greenberg J. T. and Ausubel F. M. (1993) *Arabidopsis* mutants compromised for the control of cellular damage during pathogenesis and aging. *Plant J*. 4: 327-341

Guiamet, J. J., Tyystjarvi E., Tyystjarvi, T, John, I., Kairavuo, M., Pichersky, E. and Nooden, L. D. (2002) Photoinhibition and loss of photosystem II reaction centre proteins during senescence of soybean leaves. Enhancement of photoinhibition by the 'stay-green' mutation *cytG*. *Physiol. Plant*. 115: 468-478

Heins L, Mehrle A, Hemmler R, Wagner R, Kuchler M, Hormann F, Sveshnikov D, Soll J. (2002) The preprotein conducting channel at the inner envelope membrane of plastids. *EMBO J.* 21:2616-2625.

Hellens, R. P., Edwards, E. A., Leyland, N. R., Bean, S. and Mullineaux, P. M. (2000a) pGreen: a versatile and flexible binary Ti vector for *Agrobacterium*-mediated plant transformation *Plant Mol. Bio.* **42**: 819-832.

Hellens, R, Mullineaux, P. and Klee, H. (2000b) A guide to *Agrobacterium* binary Ti vectors *Trends in Plant Science*, **5:10:** 446-451.

Hörtensteiner, S., Vicentini, F. and Matile, P. (1995) Chlorophyll breakdown in senescent leaves: enzymatic cleavage of pheophorbide *a in vitro.* *New Phytol.* 129: 237-246

Hörtensteiner, S, Wüthrich, K. L., Matile, P., Ongania, K.-H. and Kutler (1998) The key step in chlorophyll breakdown in higher plants: cleavage of pheophorbide *a* macrocycle by a monooxygenase. *J. Biol. Chem*. 273: 15335-15339

Hu G, Yalpani N, Briggs SP, Johal GS. (1998) A porphyrin pathway impairment is responsible for the phenotype of a dominant disease lesion mimic mutant of maize. *Plant Cell* 10:1095-1105.

Ito, H., Tanaka, Y., Tsuji, H and Tanaka, A. (1993) Conversion of chlorophyll *b* to chlorophyll *a* by isolated cucumber etioplasts. *Arch. Biochem. Biophys*. 306: 148-151

Ito, H., Takaichi, S., Tsuji, H., and Tanaka, A. (1994) Properties of synthesis of chlorophyll *a* from chlorophyll *b* in cucumber etioplasts. *J. Biol. Chem*. 269: 22034-22038

Ito, H., Ohtsuka, T. and Tanaka, A. (1996) Conversion of chlorophyll *b* to chlorophyll *a* via 7-hydroxymethyl chlorophyll. *J. Biol. Chem*. 271: 1475-1479

Jacob-Wilk, D., Holland, D., Goldschmidt, E. E., Riov, J. and Eyal, Y. (1999) Chlorophyll breakdown by chlorophyllase: Isolation and functional expression of the Chlase1 gene from ethylene-treated Citrus fruit and its regulation during development. *Plant J*. 20: 653-661

Jonker, J.W., Buitelaar, M., Wagenaar, E., Van Der Valk, M.A., Scheffer, G.L., Scheper, R.J., Plosch, T., Kuipers, F., Elferink, R.P., Rosing, H., Beijnen, J.H. and Schinkel, A.H. (2002) The breast cancer resistance protein protects against a major chlorophyll-derived dietary phototoxin and protoporphyria. *Proc Natl Acad Sci U S A*. 99: 15649-15654

Kroll, D, Meierhoff, K, Bechtold, N, Kinoshita, M, Westphal, S, Vothknecht, U. C., Soll, J. and Westhoff, P. (2001) *VIPP1*, a nuclear gene of *Arabidopsis thaliana* essential for thylakoid membrane formation. *Proc Natl Acad Sci U S A*. 98: 4238-4242

Kruse, E., Mock, H-P. and Grimm, B (1995) Reduction of coproporphyrinogen oxidase level by antisense RNA synthesis leads to de-regulated gene expression of plastid proteins and affects the oxidative stress defense system. *EMBO J.* 14: 109-116

Kuchler M, Decker S, Hormann F, Soll J, Heins L. (2001) Protein import into chloroplasts involves redox-regulated proteins. *EMBO J.* 15;21:6136-6145

Mach, J. M., Castillo, A. R., Hoogstraten, R., and Greenberg, J. T., (2001) The *Arabidopsis*-accelerated cell death gene *ACD2* encodes red chlorophyll catabolite reductase and supresses the spread of disease symptoms. *Proc. Natl. Acad. Sci. USA*, 98: 771-776

Matile , P., Hörtensteiner, S., Thomas, H. and Kräutler, B. (1996) Chlorophyll breakdown in senescent leaves. *Plant Physiol.* 112: 1403-1409

Matile, P and Schellenberg, M (1996) The cleavage of phaeophorbide *a* is located in the envelope of barley gerontplasts. *Plant Physiol. Biochem*. 34: 55-59

Matile, P. and Hörtensteiner, S. (1999) Chlorophyll degradation. *Annu. Rev. Plant Physiol. Plant Mol. Biol.* 50: 67-95

Mason, J. R. and Cammack, R. (1992) The electron-transport proteins of hydroxylating bacterial dioxygenases. *Annu. Rev. Microbiol.* 46: 277-305

Mock, H-P and Grimm B. (1997) Reduction of uroporphyrinogen decarboxylase by antisense RNA expression affects activities of other enzymes involved in tetrapyrrole biosynthesis and leads to light-dependent necrosis. *Plant Physiol.* 113: 1101-1112

Oster, U., Tanaka, R, Tanaka, A. and Rüdiger, W. (2000) Cloning and functional expression of the gene encoding the key enzyme for chlorophyll *b* biosynthesis (CAO) from *Arabidopsis thaliana*. *Plant J.* 21: 305-310

Papenbrock, J., Mishra, S., Mock, H.P., Kruse, E., Schmidt, E.K., Petersmann, A.,

Braun, H.P. and Grimm, B. (2001) Impaired expression of the plastidic ferrochelatase by antisense RNA synthesis leads to a necrotic phenotype of transformed tobacco plants. *Plant J*. 2001 28:41-50

Rathinasabapathi, B, Burnet, M, Russell, B.L., Gage, D.A., Liao, P.C., Nye, G.J., Scott, P., Golbeck, J.H. and Hanson, A.D. (1997) Choline monooxygenase, an unusual iron-sulfur enzyme catalyzing the first step of glycine betaine synthesis in plants: prosthetic group characterization and cDNA cloning. *Proc Natl Acad Sci U S A.* 94: 3454-3458

Reumann S. and Keegstra K. (1999) The endosymbiotic origin of the protein import machinery of chloroplastic envelope membranes. *Trends Plant Sci.* 4: 302-307

Reyes-Arribas T, Barrett, J. E., Huber, D. J., Nell, T. A. and Clark, D. G. (2001) Leaf senescence in a non-yellowing cultivar of chrysanthemum (*Dendranthema grandiflora*) *Physiol. Plant.* 111: 540-544

Rodoni, S., Vicentini, F., Schellenberg, M., Matile, P. and Hörtensteiner, S. (1997) Partial purification of red chlorophyll catabolite reductase, a stroma protein involved in chlorophyll breakdown. *Plant Physiol.* 115: 677-682

Saitou, N. and Nei, N (1987) The neighbor-joining method: A new method for reconstructing phylogenetic trees. *Mol. Biol. Evol.* 4: 406-425

Scheumann, V., Helfrich, M., Schoch, S. and Ruediger, W. (1996) Reduction of the formyl group of zine pheophorbide *b in vitro and in vivo*: A model for the chlorophyll *b* to *a* transformation. *Z. Naturforsch*. 51c: 185-194

Scheumann, V., Schoch, S. and Ruediger, W., (1998) Chlorophyll *a* formation in the chlorophyll *b* reductase reaction requires reduced ferredoxin. *J. Biol. Chem.* 273: 35102-35108

Schmidt, C. L. and Shaw, L. (2001) A comprehensive phylogenetic analysis of Rieske

and Rieske-type iron-sulfur proteins. *J Bioenerg Biomembr.* 33: 9-26.

Shioi, Y., Tomita, N., Tsuchiya, T. and Takamiya, K. (1996) Conversion of chlorophyllide to pheophorbide by Mg-dechelating substrate in extracts of *Chenopodium album.* *Plant Physiol. Biochem.* 34: 41-47

Takamiya, K., Tsuchiya, T. and Ohta, H. (2000) Degradation pathway(s) of chlorophyll: what has gene cloning revealed? *Trends Plant Sci*. 5: 426-430

Tanaka, A., Ito, H., Tanaka, R., Tanaka, N.K., Yoshida, K. and Okada, K. (1998) Chlorophyll *a* oxygenase (CAO) is involved in chlorophyll *b* formation from chlroophyll *a.* *Proc Natl Acad Sci* 95: 12719-12723

Thomas H, Bortlik K, Rentsch D, Schellenberg M, and Matile P. (1989) Catabolism of chlorophyll *in vivo*: significance of polar chlorophyll catabolites in a non-yellowing senescence mutant of *Festuca pratensis.* *New Phytologist* 111: 3-8

Thomas H and Howarth C. J. (2000) Five ways to stay green. J. Exp. Bot. 51: 329-337

Thomas H, Ougham H, Canter P and Donnison I (2002) What stay-green mutants tell us about nitrogen remolilization in leaf senescence. *J. Exp. Bot.* 53: 801-808

Thompson,J.D., Gibson,T.J., Plewniak,F., Jeanmougin,F. and Higgins,D.G. (1997) The ClustalX windows interface: flexible strategies for multiple sequence alignment aided by quality analysis tools. *Nucleic Acids Research,* 24:4876-4882

Tsuchiya, T., Ohta, H., Katsuya, O., Iwamatsu, A., Shimada, H., Masuda, T. and Takamiya, K. (1999) Cloning of chlorophyllase, the key enzyme in chlorophyll degradation: Finding of a lipase motif and the induction by methyl jasmonate. *Proc. Natl. Acad. Sci. USA* 96 : 15362-15367

Vicentini F, Hoertensteiner S, Schnellenberg M, Thomas H and Matile P (1995a) Chlorophyll breakdown in senescent leaves: identification of the biochemical lesion in a

stay-green genotype of *Festuca pratensis* Huds. *New Phytologist* 129: 247-252

Vicentini, F., Iten, F. and Matile, P. (1995b) Development of an assay for Mg-dechelatase of oilseed rape cotyledons, using chlorophyllin as the substrate. *Physiol. Plant.* 94: 57-63

Wüthrich, K. L., Bovet, L., Hunziker, P. E., Donnison, I. S. and Hörtensteiner, S. (2000) Molecular cloning, functional expression and characterisation of RCC reductase involved in chlorophyll catabolism. *Plant J.* 21: 189-198

Zapata, M., Rodriguez, F. and Garrido, J. L. (2000) Separation of chlorophylls and carotenoids from marine phytoplankton: a new HPLC method using a reversed phase C8 column and pyridine-containing mobile phases. *Marine Ecol. Prog. Ser.* 195: 29-45

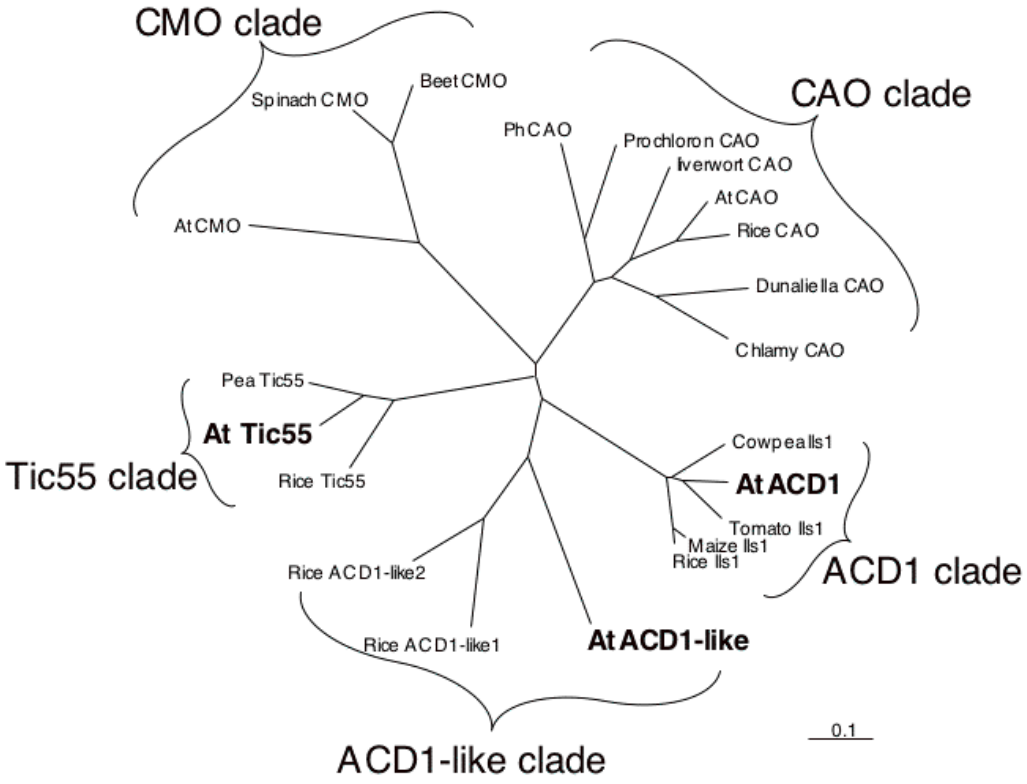

Figure 1 R. Tanaka

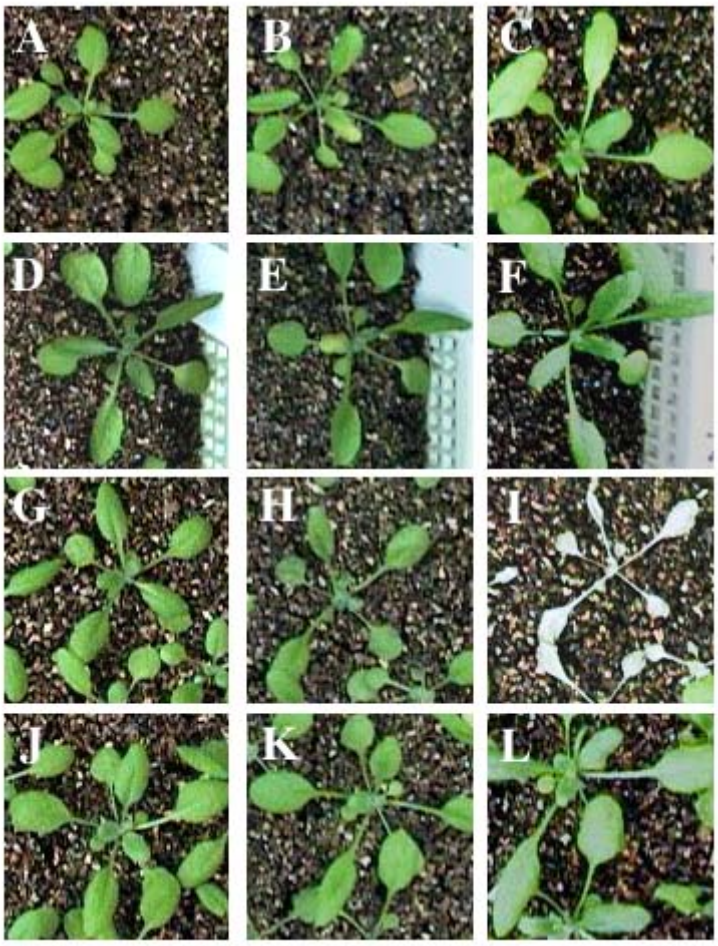

Figure 2 R. Tanaka

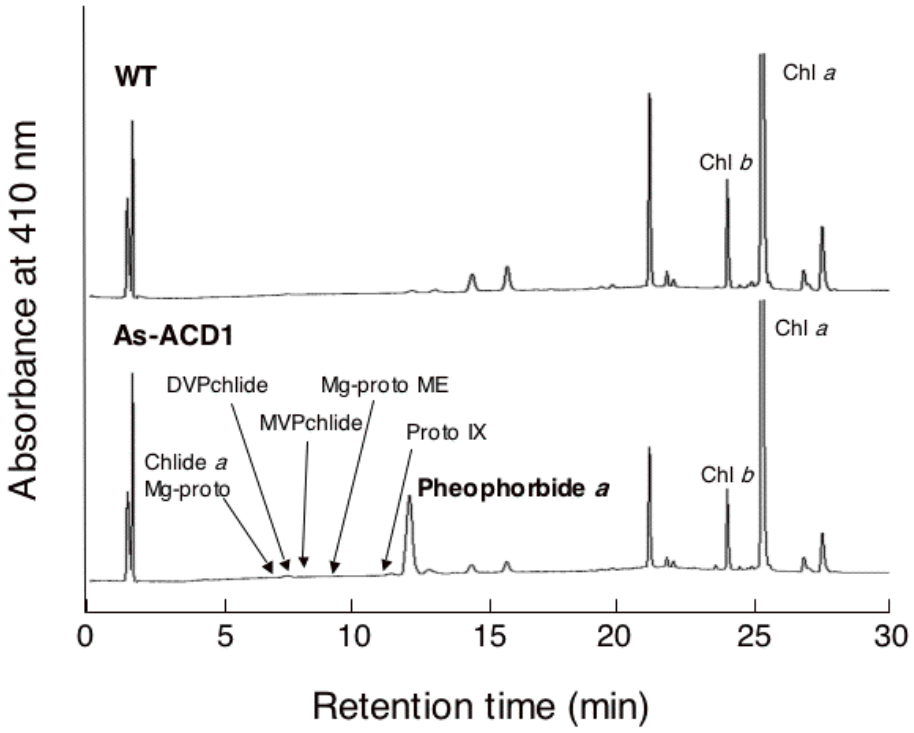

Figure 3 R. Tanaka

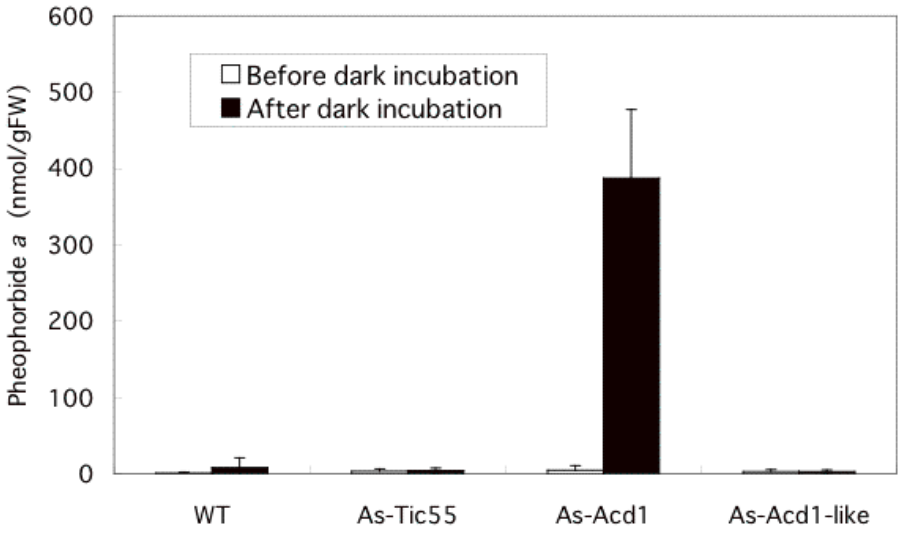

Figure 4　R. Tanaka

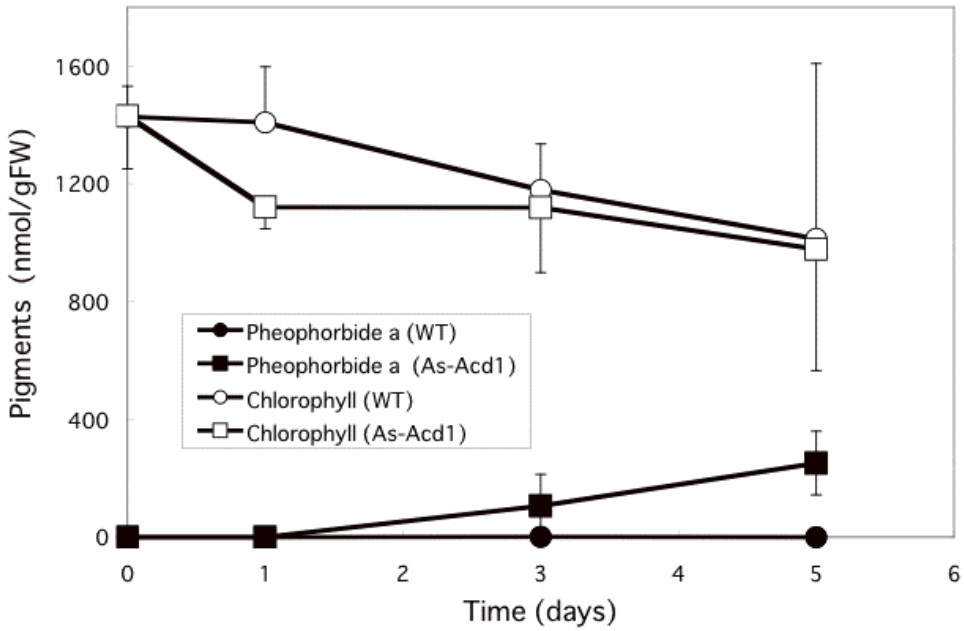

Figure 5　R. Tanaka

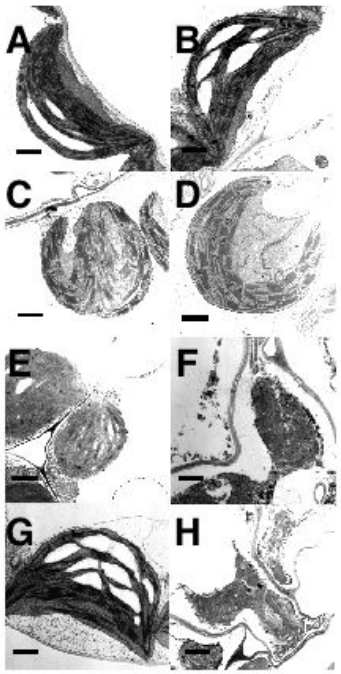

Figure 6 R. Tanaka